2018 15th International Conference on Ubiquitous Robots (UR)
Hawaii Convention Center, Hawai'i, USA, June 27-30, 2018

Environment-Dependent Modulation of Human Ankle Stiffness and its Implication for the Design of Lower Extremity Robots

Varun Nalam and Hyunglae Lee, *Member, IEEE*

***Abstract* — Understanding how human ankle mechanics are modulated during interaction with a wide range of environments is essential to develop reliable and robust lower extremity robots such as prosthetics and exoskeletons that mimic the behavior of the human ankle. This paper investigates the effect of mechanical environment on the modulation of human ankle stiffness and its underlying mechanisms. A novel multi-axis robotic platform, capable of actuating the ankle in both dorsiflexion−plantarflexion (DP) and inversion−eversion (IE), was used to quantify ankle stiffness in 2 degrees-of-freedom, while human subjects maintain upright posture in a range of stiffness-defined haptic environments. Ankle stiffness in DP increased with increasing compliance of haptic environment, but it was significantly lower than the stiffness measured in a rigid mechanical environment. On the other hand, ankle stiffness in IE was relatively constant in both compliant and rigid environments. Analysis of muscle activation and center of pressure of the ground reaction force provided an explanation for the underlying mechanisms of these observations. Notably, the analysis confirmed that modulation of ankle stiffness cannot be solely explained by activation of superficial ankle muscles. Implications for the design and control of lower extremity robots mimicking human ankle impedance are discussed.**

I. Introduction

Lower extremity robots have gained increasing utility in various fields including industrial, military, and clinical applications, both for performance enhancement and restoration [1]. For such devices, proper control of the robotic ankle joint in accordance with human ankle behavior is essential to achieve seamless and stable interaction of the human-robot system at the interface with the physical environment. As an important step to this goal, it is imperative to understand how human ankle mechanics are modulated and controlled during interaction with a wide range of environments. This knowledge would aid in developing reliable and robust robotic controllers that can effectively mimic the behavior of the human ankle.

Considerable efforts have been made to integrate human ankle behavior into the design and control of the ankle joint of the lower extremity robots such as exoskeletons, active ankle-foot orthoses, and prostheses. Imitating the torque profile of the human ankle during locomotion on a flat rigid surface has been one of the most popular approaches [2-4]. However, performance of robots that utilize this approach may be significantly compromised when interacting with more complex environments, such as a carpeted floor or rough terrain.

Several attempts have been made to design robotic controllers suitable for a wider range of tasks. Quasi-static impedance models were developed for each sub-phase of gait by approximating the torque-angle relationship at the ankle [5-8]. However, since human ankle mechanics are dynamically modulated during gait, the quasi-static approach cannot be an optimal solution. Adaptive and iterative methods have been proposed to improve performance for various tasks [9, 10], but these approaches are highly subject and task-dependent and require extensive training. Neuromuscular model-based controllers have also recently gained prominence. Simplified muscle models and reflex models were developed to mimic human ankle behavior [11-14]. However, each of these models addressed only a specific functionality of the overall ankle behavior.

In an effort to better model human ankle mechanics, ankle impedance, the dynamic relationship between ankle kinematics and kinetics, has been investigated. Earlier studies were performed in static task conditions, for example in seated [15, 16] or supine positions [17], limiting their application to dynamic functional tasks. The use of a wearable ankle robot enabled the characterization of ankle impedance during dynamic tasks, for example, locomotion [18, 19]. However, the wearable ankle device did not allow for the characterization when the loading at the ankle is substantial, such as during stance phase of locomotion or dynamic postural balance in standing.

In order to address the above limitations, two recent studies have proposed robotic ankle platforms [20, 21]. Rouse et al. developed a 1 degree-of-freedom (DOF) robotic platform to characterize ankle impedance during stance phase of walking. Ficanha et al. have extended this study and proposed a 2-DOF robotic platform to characterize ankle impedance in both dorsiflexion−plantarflexion (DP) and inversion−eversion (IE). However, because each of the platforms operated in a single control mode, either in a position control mode [20] or a torque control model [21], characterizations were strictly limited to a single mechanical environment.

We recently developed a multi-axis robotic platform capable of simulating a wide range of realistic mechanical (haptic) environments as well as providing fast and precise perturbations to the ankle in 2 DOFs, i.e., DP in the sagittal

Varun Nalam is with the School for Engineering of Matter, Transport, and Energy, Arizona State University, Tempe, AZ 85287, USA (e-mail: varun.nalam@asu.edu).

Hyunglae Lee is with the School for Engineering of Matter, Transport, and Energy, Arizona State University, Tempe, AZ 85287, USA (corresponding author: 480-727-7463; fax: 480-727-9321; e-mail: hyunglae.lee@asu.edu).

This study was completed by a support of Virginia G. Piper Foundation, adidas-ASU Global Sport Alliance, and Ira A. Fulton Schools of Engineering at the Arizona State University.

plane and IE in the frontal plane [22]. Thus, this new platform allows us to seamlessly quantify multi-dimensional ankle mechanics, including ankle impedance, while humans perform various lower extremity tasks in realistic physical environments.

In this study, we utilized this multi-axis robotic platform to investigate how ankle stiffness is modulated and controlled when humans maintain upright posture against a wide range of mechanical environments, from compliant to rigid environments. As our ultimate goal is to develop a robust and effective model of ankle impedance for the robotic controller to be used in lower extremity robots such as exoskeletons and prostheses, it is important to identify underlying mechanisms of this environment-dependent modulation. To this end, we investigated how muscle activation and center of pressure of the ground reaction force (CoP) contributed to the modulation of ankle stiffness.

II. Methods

A. Experimental Setup

The experimental setup was designed to quantify multi-dimensional ankle stiffness, specifically, DP stiffness in the sagittal plane and IE stiffness in the frontal plane, while human subjects maintain upright standing posture in a range of mechanical environments. It consisted of the multi-axis robotic platform, a weight scale, a dual-axis goniometer, surface EMG sensors, a body weight support, and a visual feedback display (Fig. 1).

Subjects stood upright with the right foot on the robotic platform and the left foot on the weight scale besides the platform. Ankle torques and CoP were calculated from the force plate (9260AA3, Kistler, NY), and ankle angles were measured using the goniometer (SG 110, Biometrics Ltd, UK). Muscle activation was measured using surface EMG sensors (Trigno EMG systems, Delsys, MA), attached to the belly of four major ankle muscles: Tibialis anterior (TA), soleus (SOL), peroneus longus (PL), and medial gastrocnemius (GAS) muscles. To ensure safety, each subject wore a harness attached to a body weight support system (LiteGait, AZ).

The visual feedback displayed the target and current levels of three parameters to be controlled by subjects: weight distribution between both legs, CoP displacements in both DP and IE directions, and TA muscle activation. The weight distribution feedback was used to ensure constant loading at the ankle throughout the study. The combination of CoP and TA muscle activation feedbacks allowed subjects to effectively control the degree of co-contraction of ankle muscles.

The platform was operated in two control modes: haptic control and position control modes. The haptic controller, which was based on the admittance control scheme [23], was implemented to simulate a wide range of stiffness-defined haptic environments. For the quantification of ankle stiffness, the position controller applied ramp-and-hold perturbations (an amplitude of 3° and a speed of 40°/s) to the ankle. The control mode could be switched within 0.5 ms, which ensured

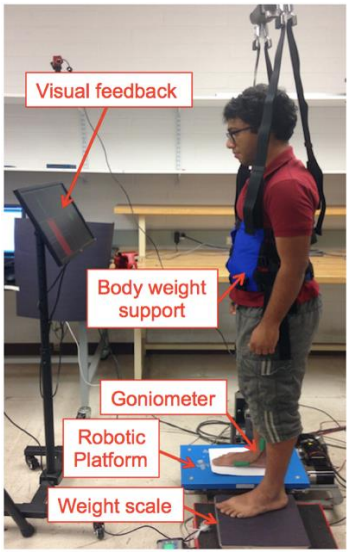

Fig.1 The experimental setup for posture maintenance in upright standing.

seamless quantification of ankle stiffness while subjects interacted with haptic environments [22]. The controllers were implemented using a Simulink real time system on a PCM 3356 (Advantech, Taiwan).

B. Subjects

Five healthy male individuals with no reported history of neurological disorders or orthopedic limitations were recruited for this study. The subjects were from ages ranging 18−28, height ranging 170−191 cm, and weight ranging 56−85 kg. This study was approved by the Institutional Review Board of Arizona State University and all experiments were performed after informed consent of the subjects.

C. Experimental Protocol

Each subject participated in two sets of experiments. In the first experiment, the subject interacted with environments having different levels of compliance in order to investigate the environment-dependent modulation of human ankle stiffness. In the second experiment, the subject maintained upright posture in a rigid environment with different levels of muscle co-activation in order to analyze the underlying mechanisms of stiffness modulation.

Prior to the main experiments, the weight distribution between both legs, and the CoP about the right leg were measured during quiet standing. In addition, the maximum voluntary contraction (MVC) of each of the four muscles controlling the ankle was recorded. These three data were used both for visual feedback and for post-experiment analysis.

In the first experiment (compliant trials), the subject was instructed to maintain upright posture in the simulated compliant environments. Three different levels of compliant environments were simulated in each DOF of the ankle. The simulated stiffness values of the platform in DP were 50,

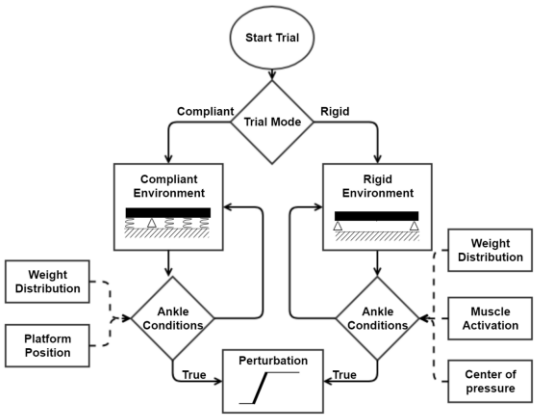

Fig.2 The flowchart of the experimental protocol consisting of compliant and rigid trials. The perturbations were applied to the ankle only if specific conditions are satisfied for a time interval of 0.5 sec.

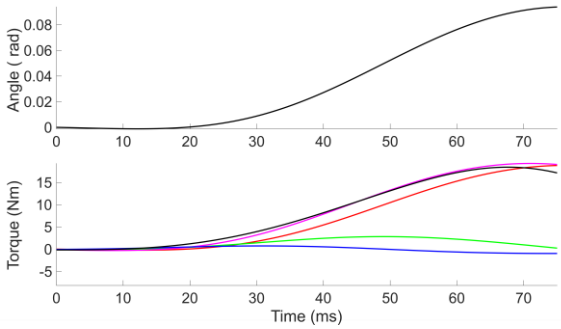

Fig.3 A representative quantification of ankle impedance obtained by regression. (Top) The position profile of the perturbation. (Bottom) The torque responses. Red, green and blue denote the contribution of stiffness, damping, and inertia. Measured torque (black) matched well with the estimated torque (magenta) by summing the torque contributions of three ankle parameters.

150, 450 Nm/rad, while the values in IE were 16.7, 50, 150 Nm/rad. These values were selected so that the ankle could be exposed to different haptic conditions ranging from approximately one third to three times the ankle stiffness in that particular DOF. The damping ratio of 0.6 was chosen to ensure a slightly underdamped platform. In addition, the lowest possible inertia that could be achieved without affecting the stability of the platform was simulated: 0.6 kgm^2 in DP and 0.15 kgm^2 in IE. When a compliant environment was simulated in one DOF, a rigid environment was implemented in the other DOF so that subjects can focus on posture control in the DOF of interest.

A brief ramp-and-hold perturbation was applied to the ankle when the subject maintained the platform in a horizontal position (±0.3°) and equal weight distribution between the legs (±1.5% of body weight) for 0.5s (Fig. 2). Perturbations were applied in dorsiflexion, inversion, and eversion in a random order. Platarflexion perturbations were not used due to possible loss of contact between the platform and the foot. The perturbation amplitude was set to 3° with a duration of 75ms. This short duration of perturbation allows for the accurate quantification of intrinsic ankle stiffness with no influence of reflex responses. Ten repeated trials were completed for each of 9 experimental conditions: 3 stiffness levels x 3 perturbation directions. A total of 90 trials were split into 9 blocks, and each block was randomized with regard to the order of simulated stiffness and perturbation direction.

In the second experiment (rigid trials), the subject stood upright on a rigid platform and was instructed to maintain the following three conditions: equal weight distribution between the legs (within ±1.5% of the body weight), CoP within ±2% of the pre-recorded value, and TA muscle activation within ±2 %MVC of the target activation level (Fig. 2). Target muscle activation levels for TA were selected as 0, 10, 20 %MVC. When these three conditions were satisfied for 0.5s, the same perturbations described in the first experiment were triggered. Ten repeated trials were completed for each of 9 experimental conditions: 3 muscle activation levels x 3 perturbation directions. A total of 90 trials were split into 9 blocks, and each block was randomized with regard to the order of perturbation direction.

D. Data Processing and Analysis

Data from the force plate and the goniometer were collected using a DX-32 AT DAQ (Diamond Systems, CA) at a sampling frequency of 2 kHz and filtered using a 4^{th} order Butterworth low-pass filter having a cut-off frequency of 20 Hz. Ankle torques about DP and IE axes were calculated using the normal and shear forces recorded from the force plate, and ankle kinematics were obtained from the filtered goniometer data. In calculating ankle torques, torques due to platform dynamics were first identified under no loading condition and subtracted from the measured torques in human experiments.

Ankle stiffness was calculated by fitting a 2^{nd} order model, consisting of ankle stiffness, ankle damping, and foot inertia, to the measured ankle kinematics and torques. Linear regression was performed over an interval of 75 ms (the duration of the perturbation) and 55 ms in identifying the parameters in DP and IE, respectively. A shorter interval was used for the identification in IE to minimize the effect of linear motion at the ankle due to misalignment between the ankle axis and the axis of rotation of the robotic platform. To check the reliability of parameter identification, the percentage variance accounted for (%VAF) between the measured ankle torque and the estimated ankle torque calculated from the identified stiffness, damping, and inertia was calculated.

Surface EMG signals were band-pass filtered between 20 and 450 Hz and sampled at 2 kHz. The filtered signals were centered, rectified, and normalized by the pre-recorded MVC. To investigate the contribution of muscle activation to the modulation of ankle stiffness, the average EMG activity was calculated over an interval of 100 ms just before the perturbation.

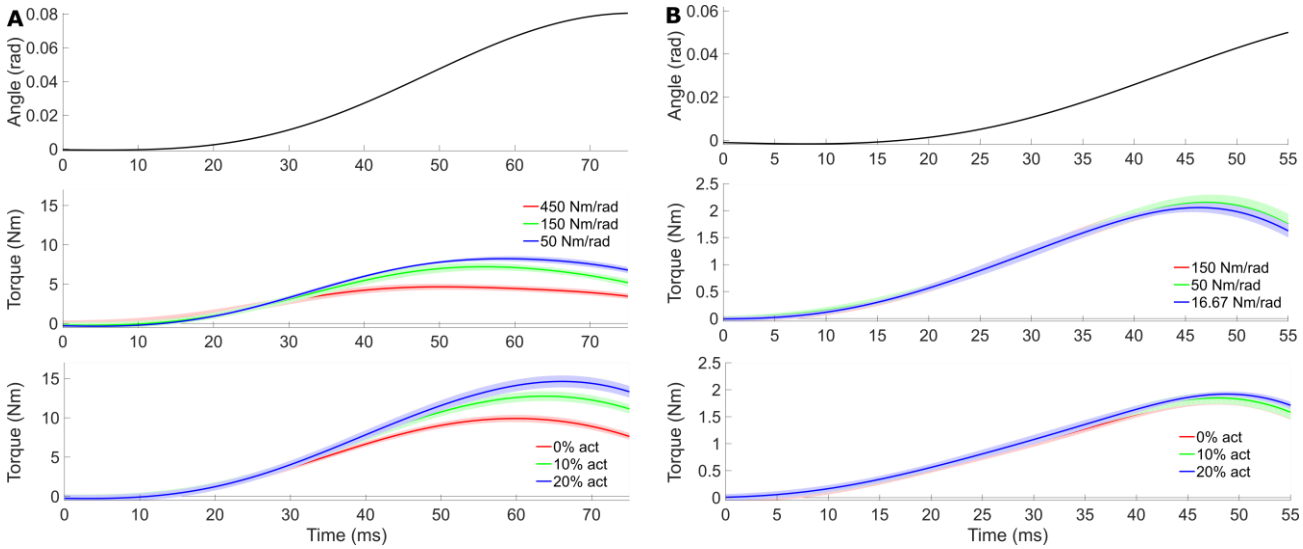

Fig.4 Torque measurements in response to the ramp-and-hold position perturbation (top). Torq ue responses in the first experiment (compliant trials; mid row). Torque responses in the second experiment (rigid trials; bottom row). **A:** DP, **B**: IE. The red, green and blue lines show the torque responses during different trials. The mean (solid) and 1 standard deviation (shaded) of all subjects are presented.

TABLE I. RELIABILITY MEASURES OF REGRESSION

Trials	DP		IE	
	Stiffness (Nm/rad)/ %MVC	%VAF	Stiffness (Nm/rad)/ MVC	%VAF
Compliant	450	93.3 (3.1)	150	97.6 (1.4)
	150	97.2 (1.9)	50	97.9 (1.3)
	50	96.4 (2.6)	16.7	97.8 (1.6)
Rigid	0	98.4 (0.4)	0	98.4 (0.7)
	10	99.2 (0.1)	10	98.5 (0.6)
	20	99.3 (0.1)	20	98.6 (0.5)

For each DOF of the ankle, ankle stiffness was compared over 3 different compliant environments, and these results were further compared with ankle stiffness identified in the rigid environment. This analysis allowed us to determine the effect of environmental mechanics on the modulation of ankle stiffness. To understand the underlying mechanisms contributing to the modulation of ankle stiffness during interaction with various environments, an additional analysis was performed that investigated EMG activity and CoP before perturbation.

III. RESULTS

A. *Reliability of Stiffness Identification*

Based on precise torque and kinematic measurements, the proposed robotic approach could reliably identify ankle stiffness in both DOFs in all experimental conditions (Fig. 3 and 4). When subjects interacted with a range of compliant environments in the first experiment, the %VAF was higher than 93.3% and 97.6% for DP and IE, respectively. During interaction with a rigid surface in the second experiment, the %VAF was higher than 98.4% for both DP and IE and for all muscle activation levels (Table I).

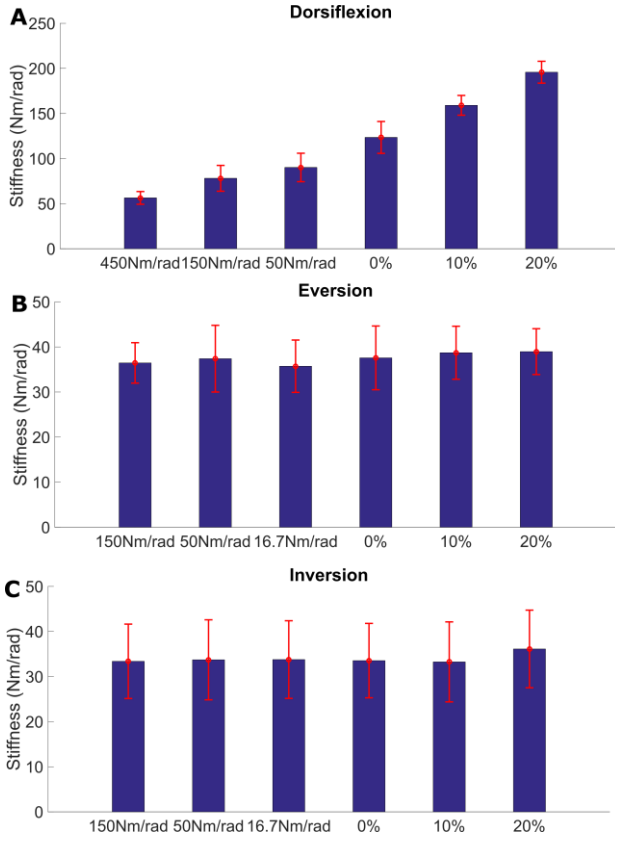

Fig.5 Ankle stiffness in compliant and rigid environments. A: dorsiflexion, B: eversion, C: inversion.

B. *Ankle Stiffness in Compliant Environments*

Ankle stiffness in DP was modulated in an environment-dependent manner (Fig. 5). It linearly increased (from 56.4 to

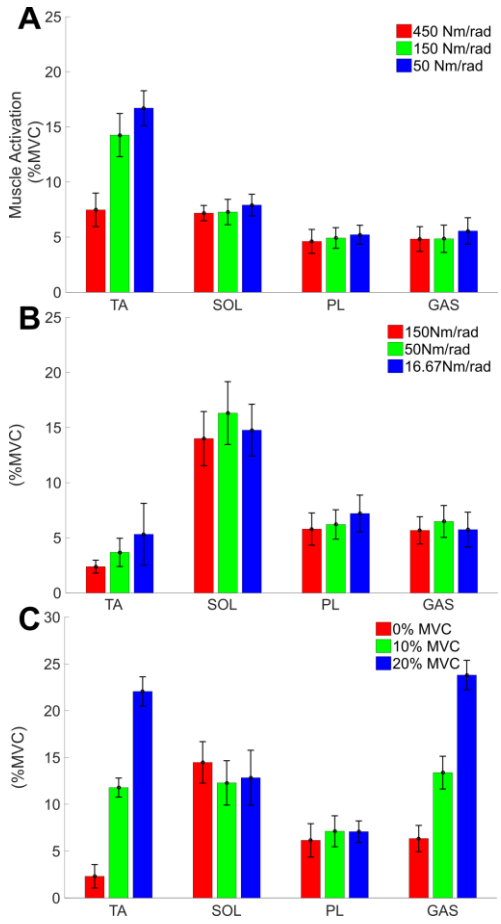

Fig.6 Muscle activation prior to the perturbation during (**A**) compliant dorsiflexion trials, (**B**) compliant IE trials, and (**C**) rigid trials.

90.1 Nm/rad) with increasing compliance (from 450 to 50 Nm/rad) of haptic environment (Fig. 5A). On the other hand, ankle stiffness in IE was not affected by the compliance of haptic environment (Fig. 5B and 5C).

C. Ankle Stiffness in a Rigid Environment

Co-contraction of TA and its antagonistic muscles (plantarflexors) effectively increased ankle stiffness in DP (Fig. 5A). It linearly increased (from 123.4 to 195.8 Nm/rad) with increasing muscle co-contraction (0 to 20 %MVC). Notably, the range of stiffness observed in rigid trials was significantly higher than that observed in compliant trials. Even the lowest stiffness (123.4 Nm/rad) measured during quiet standing (0 %MVC) in a rigid environment was greater than the highest stiffness (90.1 Nm/rad) measured in the most compliant environment (50 Nm/rad). In contrast, ankle stiffness in IE was relatively invariant regardless of muscle co-contraction levels (Fig. 5B and 5C).

D. EMG and CoP Analysis

Ankle stiffness in DP increased with TA muscle activation in both compliant and rigid experiments, but the amount of increase was greater in the rigid experiment. While GAS predominantly provided co-contraction in the rigid experiment, it did not change significantly (about 5 %MVC across compliant trials) in the compliant experiment (Fig. 6). This partly explained why ankle stiffness in DP was significantly lower during interaction with compliant environments.

TABLE II. POSITION OF CENTER OF PRESSURE

Trials	DP		IE	
	Stiffness (Nm/rad)/ %MVC	CoP (mm)	Stiffness (Nm/rad)/ MVC	CoP (mm)
Compliant	450	1.41 (1.81)	150	0.23 (0.39)
	150	0.06 (0.57)	50	0.43 (0.51)
	50	0.08 (0.24)	16.7	0.42 (0.49)
Rigid	0	56.05 (14.36)	0	0.007 (0.009)
	10	53.89 (15.30)	10	0.007 (0.003)
	20	53.13 (13.96)	20	0.002 (0.003)

However, the direct comparison of EMG activity between the trials in the most compliant environment (50 Nm/rad) and the trials of quiet standing in the rigid environment (0 %MVC) confirmed that activation of major superficial ankle muscles alone was insufficient to fully explain the modulation of ankle stiffness in DP. In detail, overall EMG activity of the measured ankle muscles was greater in the compliant trials with 50 Nm/rad than the rigid trials with 0 %MVC, but ankle stiffness in DP was significantly greater (> 30 Nm/rad) in the trials with 0 %MVC. This negative correlation contradicts the well-known positive correlation between muscle activity and joint stiffness, suggesting that there exists additional factor influencing the modulation of ankle stiffness in DP.

Activation of PL muscle contributing to ankle motion in IE was rather invariant in the given experimental conditions. In the compliant experiment, even the most compliant environment (16.7 Nm/rad) did not induce significant activation of PL. In the rigid experiment, co-contraction of TA and its antagonistic muscles did not increase activation of PL. As a result, ankle stiffness in IE remained relatively constant in both compliant and rigid experiments.

Notably, significant difference in the position of CoP was observed between the compliant and rigid experiments in DP, but not in IE. In the rigid experiment, the CoP in DP direction was about 53-56 mm in front of the ankle axis (Table II). On the other hand, in the compliant experiment, the CoP was close to the ankle axis. These observations were consistent with EMG activity of GAS, being significantly greater in the rigid experiment but low in the compliant experiment. The position of CoP positively correlated with the stiffness variation found between the compliant and rigid experiments. The CoP in IE direction remained close to the ankle axis in all measurement conditions.

IV. Discussion

For lower extremity robots, such as exoskeletons, ankle foot orthoses, and prostheses, proper control of the robotic ankle joint in accordance with human ankle behavior is crucial to achieve seamless and stable interaction with the physical environment. In an effort to realize this overarching goal, in this paper, we have investigated how ankle stiffness is modulated when interacting with environments with varying compliance. To the best of our knowledge, this is the first study to investigate the effect of mechanical environment on the modulation of human ankle stiffness in the maintenance of upright posture.

Ankle stiffness in DP was modulated in an environment-dependent manner. Activation of ankle muscles contributing to DP motions and ankle stiffness in DP were highly correlated and increased with increasing compliance of environment in DP. It is presumed that co-contraction of ankle muscles is an effective way to increase ankle stiffness for the maintenance of stable upright posture especially in compliant environments, as observed in a previous upper extremity study [24].

The analysis comparing the compliant experiment with the rigid experiment confirmed that modulation of ankle stiffness in DP cannot solely be explained by activation of major superficial ankle muscles, but the combination of muscle activation and CoP (or ankle torque as it is directly related to CoP) is necessary to account for ankle stiffness in various mechanical environments. Thus, well-known stiffness models for other joints or limbs (e.g. upper arm and knee) that map joint/limb kinematics and muscle activation to joint/limb stiffness should be modified for the ankle by including an additional factor of CoP or ankle torque, as long as measurement of muscle activation relies on EMG activity of several superficial ankle muscles.

Ankle stiffness in IE was not significantly affected by changing mechanical environments. Activation of ankle muscles contributing to IE and ankle stiffness in IE didn't change with increasing compliance of environment in IE. While the consistent rule (approximately one third to three times the ankle stiffness in that particular DOF) was applied in both DOFs in selecting stiffness values of compliant environments, even the most compliant environment in IE was not challenging enough to properly increase the level of muscle activation. Further investigation with more compliant environments is warranted. In the given experimental condition, both muscle activation and CoP in IE direction were relatively constant. This further supports the dependency of ankle stiffness on both muscle activation and CoP. The results also demonstrate that the ankle stiffness is modulated independently across different axes, which allows for the design of simple modular controllers for multiple DoF prosthetic devices, exoskeletons, etc.

Results of this study will pave the way for constructing an ankle stiffness model applicable to various mechanical environments. This model will provide the basis for the design of an adaptable impedance controller of the robotic ankle joint for changing environments. Furthermore, by incorporating the findings obtained from this study, controllers can be designed separately across the DOF to control the robotic ankle impedance, due to independence in the modulation of human ankle stiffness along DP and IE. Accurate information on human ankle impedance based on kinematics, muscle activation, and kinetics (CoP) would eliminate the need for abstract learning based controllers and improve reliability without the necessity of training. It will also provide a guideline to optimize the trade-off between performance and coupled stability of the human-robot system, where accurate quantitative information on human impedance is a key factor for successful optimization.

References

[1] A. M. Dollar and H. Herr, "Lower extremity exoskeletons and active orthoses: challenges and state-of-the-art," *IEEE Transactions on robotics,* vol. 24, pp. 144-158, 2008.

[2] J. M. Caputo and S. H. Collins, "A universal ankle–foot prosthesis emulator for human locomotion experiments," *Journal of biomechanical engineering,* vol. 136, p. 035002, 2014.

[3] J. Zhang, C. C. Cheah, and S. H. Collins, "Experimental comparison of torque control methods on an ankle exoskeleton during human walking," in *Robotics and Automation (ICRA), 2015 IEEE International Conference on*, 2015, pp. 5584-5589.

[4] A. H. Hansen, D. S. Childress, S. C. Miff, S. A. Gard, and K. P. Mesplay, "The human ankle during walking: implications for design of biomimetic ankle prostheses," *Journal of Biomechanics,* vol. 37, pp. 1467-1474, 2004.

[5] J. A. Blaya and H. Herr, "Adaptive control of a variable-impedance ankle-foot orthosis to assist drop-foot gait," *IEEE Transactions on neural systems and rehabilitation engineering,* vol. 12, pp. 24-31, 2004.

[6] M. K. Shepherd and E. J. Rouse, "The VSPA Foot: A Quasi-Passive Ankle-Foot Prosthesis with Continuously Variable Stiffness," *IEEE Transactions on Neural Systems and Rehabilitation Engineering,* 2017.

[7] F. Sup, A. Bohara, and M. Goldfarb, "Design and control of a powered transfemoral prosthesis," *The International journal of robotics research,* vol. 27, pp. 263-273, 2008.

[8] A. H. Shultz, B. E. Lawson, and M. Goldfarb, "Variable cadence walking and ground adaptive standing with a powered ankle prosthesis," *IEEE Transactions on Neural Systems and Rehabilitation Engineering,* vol. 24, pp. 495-505, 2016.

[9] A. Calanca, L. Capisani, and P. Fiorini, "Robust force control of series elastic actuators," in *Actuators*, 2014, pp. 182-204.

[10] J. Bae and M. Tomizuka, "A gait rehabilitation strategy inspired by an iterative learning algorithm," *Mechatronics,* vol. 22, pp. 213-221, 2012.

[11] M. F. Eilenberg, H. Geyer, and H. Herr, "Control of a powered ankle–foot prosthesis based on a neuromuscular model," *IEEE transactions on neural systems and rehabilitation engineering,* vol. 18, pp. 164-173, 2010.

[12] J. Markowitz, P. Krishnaswamy, M. F. Eilenberg, K. Endo, C. Barnhart, and H. Herr, "Speed adaptation in a powered transtibial prosthesis controlled with a neuromuscular model," *Philosophical Transactions of the Royal Society of London B: Biological Sciences,* vol. 366, pp. 1621-1631, 2011.

[13] D. P. Ferris, J. M. Czerniecki, and B. Hannaford, "An ankle-foot orthosis powered by artificial pneumatic muscles," *Journal of applied biomechanics,* vol. 21, pp. 189-197, 2005.

[14] H. Geyer and H. Herr, "A muscle-reflex model that encodes principles of legged mechanics produces human walking dynamics and muscle activities," *IEEE Trans Neural Syst Rehabil Eng,* vol. 18, pp. 263-73, Jun 2010.

[15] H. Lee, P. Ho, M. Rastgaar, H. I. Krebs, and N. Hogan, "Multivariable Static Ankle Mechanical Impedance with Active Muscles," *IEEE Transactions on Neural Systems and Rehabilitation Engineering,* vol. 22, pp. 44-52, Jan 2014.

[16] H. Lee, H. I. Krebs, and N. Hogan, "Multivariable Dynamic Ankle Mechanical Impedance with Active Muscles," *IEEE Transactions on Neural Systems and Rehabilitation Engineering,* vol. 22, pp. 971-981, Sep 2014.

[17] R. E. Kearney and I. W. Hunter, "System-Identification of Human Joint Dynamics," *Critical Reviews in Biomedical Engineering,* vol. 18, pp. 55-87, 1990.

[18] H. Lee and N. Hogan, "Time-Varying Ankle Mechanical Impedance During Human Locomotion," *IEEE Trans Neural Syst Rehabil Eng,* vol. 23, pp. 755-64, Sep 2015.

[19] H. Lee, E. Rouse, and H. I. Krebs, "Summary of human ankle mechanical impedance during walking," *IEEE Journal of Translational Engineering in Health and Medicine,* 2016.

[20] E. J. Rouse, L. J. Hargrove, E. J. Perreault, M. A. Peshkin, and T. A. Kuiken, "Development of a Mechatronic Platform and Validation of Methods for Estimating Ankle Stiffness During the Stance Phase of Walking," *Journal of Biomechanical Engineering-Transactions of the ASME,* vol. 135, Aug 2013.

[21] E. M. Ficanha, G. Ribeiro, and M. A. Rastgaar, "Design and Evaluation of a 2-DOF Instrumented Platform for Estimation of the Ankle Mechanical Impedance in the Sagittal and Frontal Planes," *IEEE/ASME Trans on Mechatronics,* vol. 21, pp. 2531-2542, 2016.

[22] V. Nalam and H. Lee, "Design and Validation of a Multi-Axis Robotic Platform for the Characterization of Ankle Neuromechanics," in *In Proc. IEEE International Conference on Robotics and Automation*, Singapore, 2017.

[23] N. Hogan and S. P. Buerger, "Impedance and interaction control," *Robotics and Automation Handbook, New York, CRC Press,* 2005.

[24] M. A. Krutky, V. J. Ravichandran, R. D. Trumbower, and E. J. Perreault, "Interactions Between Limb and Environmental Mechanics Influence Stretch Reflex Sensitivity in the Human Arm," *Journal of Neurophysiology,* vol. 103, pp. 429-440, Jan 2010.